Chinese Chemical Letters 33 (2022) 3461–3467

Contents lists available at ScienceDirect

Chinese Chemical Letters

journal homepage: www.elsevier.com/locate/cclet

Uranium sorption on oxyhydroxide minerals by surface complexation and precipitation

Jingyi Wang, Wanqiang Zhou, Yanlin Shi, Yao Li, Dongfan Xian, Ning Guo, Chunli Liu*

Beijing National Laboratory for Molecular Sciences, Fundamental Science Laboratory on Radiochemistry and Radiation Chemistry, College of Chemistry and Molecular Engineering, Peking University, Beijing 100871, China

ARTICLE INFO

Article history:
Received 6 September 2021
Revised 29 December 2021
Accepted 10 January 2022
Available online 15 January 2022

Keywords:
Uranium mill tailings
Oxyhydroxides
Uranium sorption
Surface complexation
Surface precipitation

ABSTRACT

During the chemical weathering of the uranium mill tailings, released uranium could be immobilized by the newly formed secondary minerals such as oxyhydroxides. A deeper understanding of the interaction between uranium and common oxyhydroxides under environmental conditions is necessary. In this work, uranium sorption behaviors on Al-, Mn- and Fe-oxyhydroxide minerals (boehmite, manganite, goethite, and lepidocrocite) were investigated by batch experiments. Results showed that the uranium sorption on Al-oxyhydroxide behaved significantly differently from the other three minerals. The sorption edge of the Mn- and Fe-oxyhydroxides located around pH 5, while the sorption edge of boehmite shifted about 1.5 pH unit to near neutral. The sorption isotherms of uranium on manganite, goethite and lepidocrocite at pH 5.0 could be well fitted by the Langmuir model. Instead of surface complexation, sorption on boehmite happened mainly by uranium-bearing carbonates and hydroxides precipitation as illustrated by the characterization results. Both carbonate and phosphate strongly affected the uranium sorption behavior. The removal efficiency of uranium by boehmite exceeded 98% after three sorption-desorption cycles, indicating it may be a potential material for uranium removal and recovery.

Uranium has been used as an important resource for scientific research, nuclear energy development, and weapon production for several decades [1]. The start of uranium milling dates back to more than a hundred years ago [2], and a large amount of the excavation waste from the uranium mining and the byproducts from the reaction between uranium ores and added reagents during the leaching process has been generated [3]. These wastes, also known as uranium mill tailings, are stored at the mining sites, posing potential risks such as uranium pollution to the environment [4]. Therefore, identifying the key parameters that govern the sorption behaviors of uranium at the mill tailing disposal sites is important for understanding the migration of pollutants and designing the suitable measures for remediation.

Uranium is redox sensitive, and its most stable oxidation state in the oxidizing environments is U(VI), mainly exists as the soluble uranyl (UO_2^{2+}) species. Migration of uranium from the solid phase waste to the aqueous system mainly through the chemical weathering process [3,5,6], leading to the contamination of soils and groundwater [7–9]. Except for reducing the U(VI) to barely soluble U(IV) by reductants such as zero valent iron [10,11] or reducing bacteria [12,13], sorption by minerals and organic matters in soils and sediments is another essential route for uranium immobilization [14,15]. Recently, novel materials such as carboxyl functionalized MXene nanosheets [16], nanoporous zeolitic mineral [17] and graphene oxide nanosheets [18] have been developed for uranium removal with high sorption capacities.

The uranium deposits in northern China are mainly sandstone type [19,20], while in southeastern China are mainly granite type [21–23]. Due to the differences in mineralization and climate, the composition and weathering process of uranium mill tailings are considerably distinct from each other. However, the presence of Al, Mn and Fe are found in most of the uranium deposits, with only variations in the percentage and species [24,25]. It is observed that the migration of uranium is usually accompanied by the weathering of associated minerals [26–28], therefore it is of great importance to investigate the uranium sorption behavior on the secondary minerals such as metal oxyhydroxides, which has been found to play an important role in uranium retention [4,29,30].

Boehmite (γ-AlOOH), manganite (γ-MnOOH), goethite (α-FeOOH) and lepidocrocite (γ-FeOOH) are model minerals to study the effect of Al-, Mn- and Fe-oxyhydroxides on uranium retention. In addition to being present in the uranium mill tailings as the secondary phase [31], these minerals are found in a variety of geo-

* Corresponding author.
E-mail address: liucl@pku.edu.cn (C. Liu).

https://doi.org/10.1016/j.cclet.2022.01.019
1001-8417/

logical settings. Boehmite is assumed to be one of the most prevalent aluminum-bearing solids at Hanford site [32]. Manganite is the most stable and abundant Mn(III) oxyhydroxides [33], it was found in several nuclear waste sites [34]. Goethite is ubiquitous all over the world in soils, ores, and sediments since it is the most stable iron oxyhydroxides [35]. Lepidocrocite is the polymorph of goethite with less stability and often occurs in redoxomorphic environments [35]. These four minerals are all reported to be good adsorbents for heavy metal pollutants [36–40], but the uranium sorption behaviors on these minerals were not fully investigated except for goethite [41].

The electrostatic properties and the reactivity of uranium are influenced by its species. Factors such as pH of the solution and the co-existing anions that affect the species distribution should be considered when discussing uranium sorption behavior. The pH of the solutions around the tailings widely range from 2 to 10 since both acid and alkaline leaching are adopted in the uranium milling process based on the composition of the minerals [42–44]. Furthermore, anions such as (bi)carbonate, silicate, and sulfate are commonly seen in the *in situ* leaching of uranium milling [45] and the seepage of the tailings [46]. Phosphate is also found in several uranium tailings sites [29], and it is an effective chelating ligand used in the uranium immobilization treatment [47,48]. These anions, common in the groundwater systems [49,50], affect the species of uranium by forming stable complexes with uranyl [51–53].

Therefore, in the following work, a systematic investigation of uranium sorption behavior on the oxyhydroxide minerals (with boehmite, manganite, goethite and lepidocrocite as examples) under various solution conditions will be given by means of batch experiments. In addition, the key factors mentioned above, such as pH and anions including carbonate, phosphate, and silicate are considered.

The uranium stock solution (0.01 mol/L) used in this work was prepared by dissolving $UO_2(NO_3)_2{\cdot}6H_2O$ (A.R. grade, Sinopharm Chemical Beijing Reagent Co., Ltd) in deionized MilliQ water (18.2 MΩcm). Other chemical reagents are of analytical grade and were used without further purification. Al-, Mn- and Fe-oxyhydroxides were synthesized referring to Zhang *et al.* [54], Frierdich *et al.* [55], Schwertmann and Cornell [56], accordingly. The structure, surface property and morphology of the products before and after sorption experiments were recorded. Details of synthesis processes, characterizations, and batch experiments were listed in Supporting information.

The XRD patterns of the synthesized minerals are shown in Fig. 1. In Fig. 1a, there is no sign of the diagnostic peaks of gibbsite (*i.e.* (002), (110), and (200)) and bayerite (*i.e.*, (131)) after 80 h of hydrothermal reaction, proving that the gel precursor transformed completely to boehmite. During the synthesis process of lepidocrocite, once carbon dioxide was removed from the air before oxidation, the proportion of goethite in the final product is negligible, as shown in Fig. 1d, the (110) and (130) peak of goethite did not appear in the diffraction pattern [57].

The surface characters and structures of these synthesized minerals are detailed by SEM and TEM images in Fig. 2. The stacked boehmite nanoplates have a typical rhombic shape with a size between 50 nm to 120 nm as shown in Figs. 2a and b. In Figs. 2d and e, the synthesized manganite has a rod-like structure with a length of about 100–500 nm and a width of about 15–20 nm. In Fig. 2g, the aggregated goethite exhibits an acicular structure with a length around 0.9–1.3 μm and a width around 30–60 nm. The synthesized lepidocrocite is spindle-like as shown in Fig. 2j, the size of which is around 200–700 nm and the length/width ratio is around 8. The specific surface area (SSA) and the point of zero charge (PZC) of the synthesized minerals are listed in Table 1.

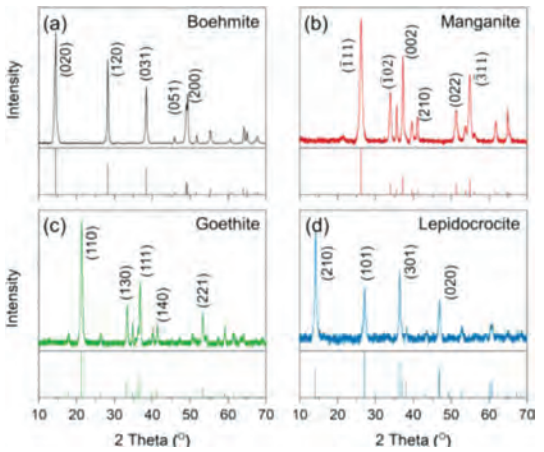

Fig. 1. XRD patterns of the synthesized minerals, all of them are in good agreement with the corresponding standard card. (a) boehmite, No. 00–021–1307, (b) manganite, No. 01–088–0649, (c) goethite, No. 00–029–0713, (d) lepidocrocite, No. 00–044–1415.

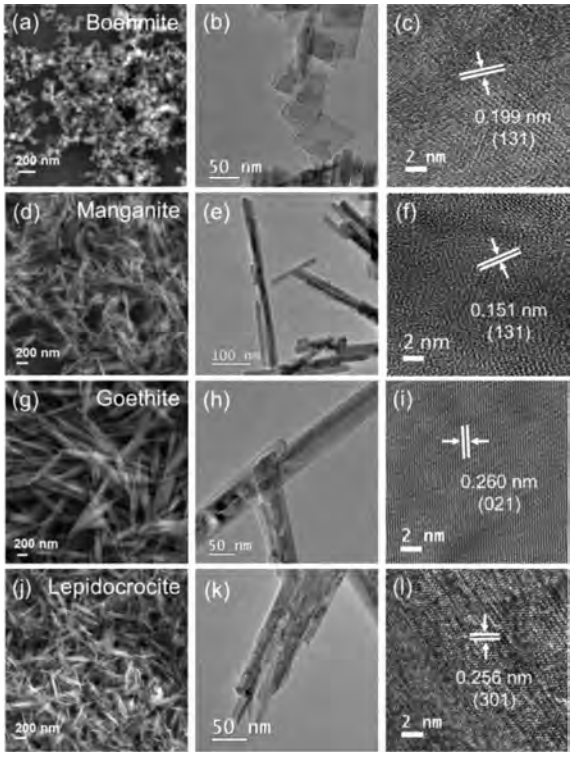

Fig. 2. SEM, TEM, and HR-TEM images of the synthesized minerals. (a-c) boehmite, (d-f) manganite, (g-i) goethite, (j-l) lepidocrocite.

To determine the suitable ratio of solid to solution for the following experiments, the sorption experiments of uranium on synthesized minerals were conducted with a sequential solid/solution ratio from 0.1 g/L to 1.5 g/L at pH 5.0. As can be seen in Fig. 3a, the sorption percentage of uranium ascended with the increasing solid/solution ratio except boehmite, which showed no significant effect on uranium sorption with its increasing solid/solution ratio. In order to clearly observe the sorption behavior of uranium on these four synthesized minerals, the solid to solution ratio was selected as 0.5 g/L according to the experimental results.

Solution pH is another important parameter to uranium sorption behaviors since it changes not only the uranium speciation in aqueous systems but also the surface binding sites of the adsorbents. The sorption edges of uranium on four synthesized minerals

Table 1
The specific surface area and the point of zero charge of the synthesized minerals.

Synthesized minerals	SSA (m^2/g)	pH_{pzc}
Boehmite	51.19 ± 0.40	6.2
Manganite	57.27 ± 0.34	5.2
Goethite	40.22 ± 0.17	6.0
Lepidocrocite	72.92 ± 0.05	6.9

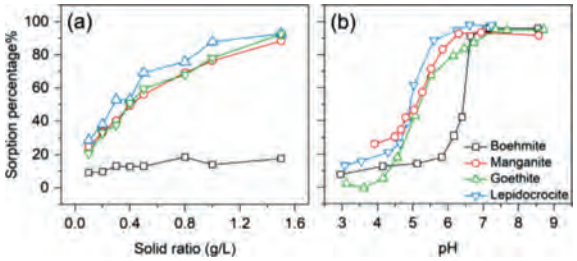

Fig. 3. Effect of solid ratio (a) and pH (b) on uranium sorption behavior on the synthesized minerals (I = 0.01 mol/L $NaClO_4$, $c(U)_{init.}$ = 11.9 mg/L, (a) pH 5.0 ± 0.1, (b) m/v = 0.5 g/L).

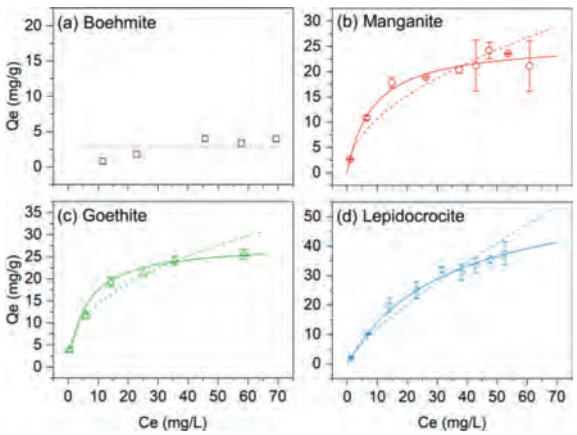

Fig. 4. The sorption isotherms of uranium on (a) boehmite, (b) manganite, (c) goethite and (d) lepidocrocite, (pH 5.0 ± 0.1, m/v = 0.5 g/L, I = 0.01 mol/L $NaClO_4$). Solid line: Langmuir model, dash line: Freundlich model, dot line: the average Q_e.

are shown in Fig. 3b. It was detected that uranium sorption percentage on boehmite increased slowly from 8% to 18% with the pH varying between 3.0 and 5.8. The sorption edge was between pH 6.2 to 7.1 as the sorption percentage increased rapidly from 31% to 96%. After that, the sorption percentage remained almost constant at high pH. Comparing to boehmite, the sorption edges of uranium on manganite, goethite, and lepidocrocite were at around pH 4 to 7. For manganite, the sorption percentage rose gradually from 26% to 93% as pH increased from 4.5 to 6.3. The sorption edge on manganite was comparable to the previous studies about uranium sorption on manganese oxides [58–60]. For goethite, between pH 4.6 and 7.3, the sorption percentage increased from 5% to 95%, similar to the results mentioned in published papers [61,62]. As for lepidocrocite, the sorption edge was within pH 4.3 and 6.3, with the sorption percentage between 21% and 95%. When the pH reached 7, all four synthesized minerals have a sorption percentage near 95%, showing an excellent sorption capacity towards uranium. This phenomenon proved the importance of pH on the uranium sorption behaviors on the synthesized minerals. Comparing to boehmite, Mn- and Fe-oxyhydroxide minerals might play a more essential role in uranium immobilization under acid conditions.

The sorption isotherms of uranium on the synthesized minerals are shown in Fig. 4, the corresponding fitting parameters of Langmuir ($Q_e = K_L Q_{max} C_e/(1 + K_L C_e)$) and Freundlich ($Qe = K_F Ce^{1/n}$)

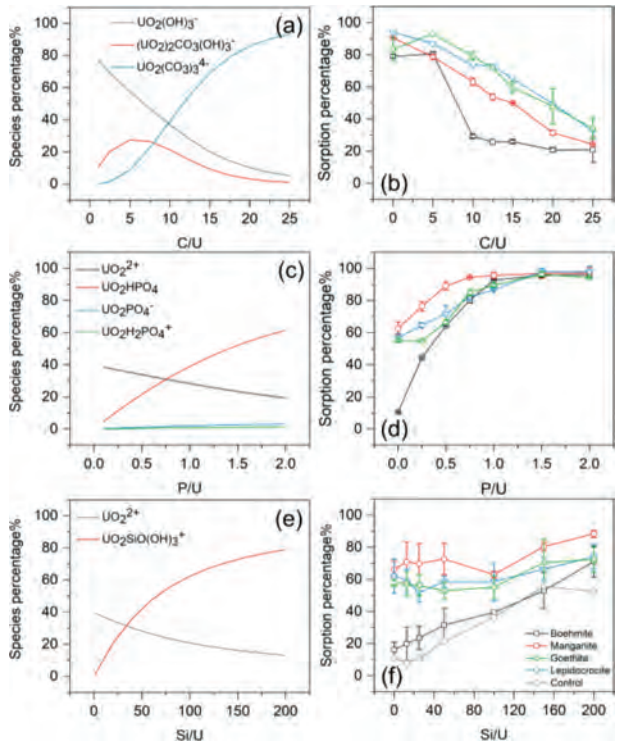

Fig. 5. Effect of anions (molar ratio) on uranium species distribution (a, c, e) and sorption behavior (b, d, f). (a, b) carbonate, pH 10.5, (c, d) phosphate, pH 5.0, (e, f) silicate, pH 5.0 (m/v = 0.5 g/L, I = 0.01 mol/L $NaClO_4$, $c(U)_{init.}$ = 11.9 mg/L).

isotherm models were obtained and listed in Table 2. Herein, Q_e (mg/g) is the uranium concentration on the adsorbent, C_e (mg/L) is the corresponding uranium concentration in the supernatant; K_L is the Langmuir sorption constant, Q_{max} (mg/g) is the maximum sorption capacity; K_F is the Freundlich sorption constant, and n is a correction factor. Due to the low sorption ability of boehmite to uranium at pH 5.0, the isotherm curve of uranium on boehmite showed a plateau across the investigated uranium concentrations as in Fig. 4a, with the average Q_e of 2.78 mg/g. However, at pH 6.7, almost all uranium in the solution was adsorbed by boehmite with the initial uranium concentration from 2.38 mg/L to 71.4 mg/L. After sorption, the concentration of uranium in the supernatant was less than 3 mg/L. The sorption mechanism of uranium on boehmite might be attributed to surface precipitation rather than complexation, and it is discussed in the following section.

As depicted in Figs. 4b-d, the sorption of uranium on the synthesized minerals can be better fitted by the Langmuir model. The maximum sorption capacity of uranium on manganite, goethite, and lepidocrocite is 25.8, 27.9 and 60.9 mg/g, respectively. If normalized by SSA, the maximum sorption density of these three minerals is 0.450, 0.694 and 0.835 mg/m^2. Therefore, the sorption capacity of uranium on the surface sites of the synthesized minerals follows the order of lepidocrocite > goethite > manganite.

The relative concentration of co-existing anions and uranyl is another essential factor in aqueous uranium speciation. Figs. 5a, c and e depict the relevant uranium species distribution with the presence of carbonate (pH 10.5), phosphate, and silicate (pH 5.0), calculated with Visual Minteq 3.1. These specific pH values were selected to ensure a higher composition of the species of interest. $UO_2(CO_3)_3^{4-}$ takes over as the main species when the C/U molar ratio reaches 10. For phosphate, the predominant species becomes UO_2HPO_4 when P/U > 0.75. Although the percentage of $UO_2PO_4^-$ and $UO_2H_2PO_4^+$ increases as phosphate concentration increases, the total amount remains less than 5%. As for silicate, the percent-

Table 2
Parameters of sorption models for uranium on synthesized minerals at pH 5.0.

Adsorbent	Langmuir model			Freundlich model		
	K_L	Q_{max} (mg/g)	R^2	K_F	n	R^2
Boehmite	–	–	–	–	–	–
Manganite	0.118 ± 0.242	25.85 ± 0.05	0.977	3.27 ± 0.58	1.95 ± 0.11	0.916
Goethite	0.166 ± 0.232	27.91 ± 0.05	0.990	5.57 ± 0.45	2.45 ± 0.07	0.977
Lepidocrocite	0.0299 ± 0.0634	60.94 ± 0.06	0.969	2.04 ± 0.30	1.30 ± 0.06	0.971

age of $UO_2SiO(OH)_3^+$ gradually rises as silicate concentration increases. The uranium sorption behavior varies with the anion concentration since the affinity of different uranium species with mineral surfaces is not the same.

Fig. 5b shows that the uranium sorption percentage on manganite, goethite, and lepidocrocite decreased almost linearly with the increase of carbonate concentration, which might be explained as that uranyl prefers to form soluble complexes with carbonate rather than surface binding sites. The sorption behavior of uranium on boehmite was another story, when the C/U was between 5 and 10, the sorption percentage dropped abruptly from 81% to 29%. This may be attributed to the dissolution of surface precipitation to soluble carbonate species. Fig. 5d indicates that a small amount of phosphate could enhance the sorption behavior of uranium to a great extent. When the P/U ratio reached 1.5, almost all uranium could be removed from the solution. Fig. 5f indicates that the effect of the silicate concentration on the uranium sorption was not apparent for the minerals other than boehmite. A control experiment without adsorbent was conducted to figure out the possible sorption mechanism. The Si concentrations in the supernatant of the control experiments remained nearly the same as it was in the initial solution, thus there were no colloids formed during the sorption experiment. Therefore, the decrease of uranium concentration in the supernatant of the control experiments was due to uranyl silicate precipitation, which was also the reason for the increased sorption percentage on boehmite. As for the minerals other than boehmite, it was the surface complexation rather than uranyl silicate precipitation that accounted for the main part of uranium removal, thus the effect of silicate on sorption was only obvious at higher silicate concentration.

Considering the studied conditions, including pH, co-existing anions and sorption isotherms, boehmite exhibited a specific behavior on uranium sorption, and quite different from the other three synthesized minerals. In the near neutral to sub-alkaline solutions, uranium could be strongly retained by boehmite. However, the sorption of uranium on boehmite was easily influenced by the solution conditions such as pH and concentration of the co-existing anions. Especially once the solution was acid or with the presence of high concentration bicarbonate, the sorption capacity of boehmite decreases significantly. Thus boehmite could be a possible candidate for uranium removal and recovery materials. Comparing to boehmite, the Mn- and Fe-oxyhydroxide minerals could be effective adsorbents for the uranium immobilization in the uranium tailings disposal sites since the surface complexation is relatively stable against pH and anions.

The mechanism of uranyl interacting with the synthesized minerals was further investigated by XPS. Samples for the XPS measurements were prepared at pH 6.7 for boehmite, and at pH 5.0 for manganite, goethite, and lepidocrocite, with the initial uranium concentration of 11.9 mg/L. In Fig. 6a, the peak at 73.8 eV is assigned to Al 2p, in agreement with previous studies [63,64]. The U $4f_{7/2}$ peak and U $4f_{5/2}$ peak can each be fitted by three peaks as shown in Fig. 6b. For U $4f_{7/2}$, the binding energies of three peaks are 380.2, 381.2 and 382.1 eV, respectively, and the corresponding proportions are 17%, 56% and 27%. The binding energies

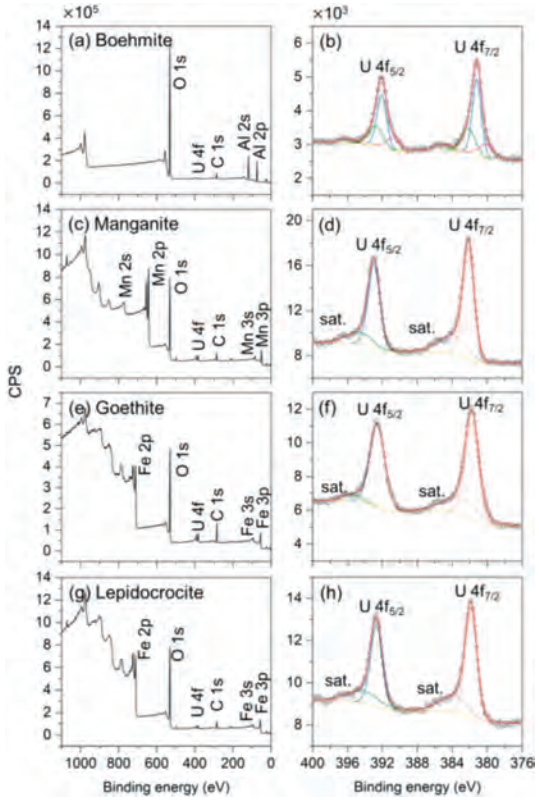

Fig. 6. XPS spectra of synthesized minerals after uranium sorption, (a, c, e, g) total survey, (b, d, f, h) high-resolution spectra of U 4f.

of U $4f_{7/2}$ are in accordance with metaschoepite or Na-substituted metaschoepite [65], while the main component shifted to a lower binding energy, which might due to the dehydration of the uranyl–hydroxy-hydrates [66]. In Fig. 6c, the splitting energy of Mn 3s doublets is regarded as the reference of Mn oxidation states [67]. Before and after uranium sorption experiments, the splitting energy of Mn 3s doublets remained unchanged at 5.5 eV. Therefore, the oxidation state of Mn in manganite was Mn(III) [68], and there were no redox reactions involved in the sorption experiments. Also, no difference in Fe 2p peaks was observed for goethite and lepidocrocite before and after uranium sorption. The binding energies of U 4f in manganite, goethite and lepidocrocite samples are above 381.7 eV as in Table 3, suggesting that uranyl was not reduced in the sorption process. In conclusion, the main mechanism for uranium sorption on boehmite was surface precipitation while on the other three synthesized minerals was surface complexation and no redox reaction was involved in the sorption process.

In consideration of the specific uranium sorption mechanism on boehmite from the other minerals, SEM and XRD were conducted to analysis the morphology and structure of the uranium-bearing precipitate on boehmite surface. Samples were prepared with a higher initial uranium concentration of 71.4 mg/L at pH 6.7.

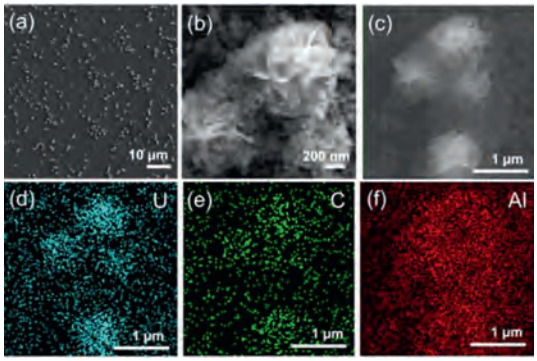

Fig. 7. (a, b) SEM images of boehmite induced uranium precipitation at pH 6.7 with the initial uranium concentration of 71.4 mg/g. (c-f) SEM-EDS element mappings of the precipitate.

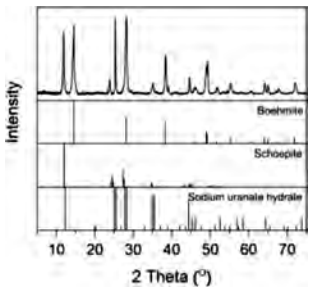

Fig. 8. XRD pattern of the precipitates on boehmite. The reference patterns are boehmite (No. 00–021–1307), schoepite (No. 00–050–1601) and sodium uranate hydrate (No. 00–012–0112).

In Figs. 7a and b, precipitate flakes formed flower-like clusters with a size of about 1 μm, covered by boehmite nanoplates. The element mapping results of the clusters are shown in Figs. 7c-f, suggesting that the precipitate might contain uranyl carbonates. In the meantime, only a small amount of uranium clusters was observed in the sample of the control experiment without minerals. The sorption percentage reached 99% for the sample with boehmite, while for the one in the control experiment was 29%. Thus, boehmite induced the effective removal of uranium from the aqueous solution by precipitation at pH 6.7.

Fig. 8 is the XRD pattern of the precipitates. Except for the diagnostic peaks of boehmite at 14.52°, 28.25° and 38.39°, the peaks at 11.89°, 23.86°, 25.32°, and 35.11° are attributed to uranyl–hydroxy-hydrates such as schoepite and sodium uranate hydrate [69], and they also contribute to the increase in the intensity of the peak at 28.25°.

Allard *et al.* investigated the uranium sorption behaviors on the Si/Al-rich gels generated from the weathering of a uranium deposits and proposed the possible mechanism of uranyl polymers co-precipitation based on the EXAFS (extensive X-ray adsorption fine structure) results [70]. They also mentioned that the sorption structure of uranium on Fe-rich gels was not the same as on the Si/Al-rich gels. The surface structure of uranium sorption on gibbsite was further discussed by Froideval *et al.* [71] and Hattori *et al.* [72] that the existence of uranyl polymers was proved by the EXAFS spectroscopy and DFT simulations. Boehmite has limited surface reactivity if well crystallized and the surface adsorptions *via* ligand exchange reactions are not likely to occur [73]. In conclusion, uranium removal by boehmite at pH 6.7 is mainly by surface precipitation rather than surface complexation, and the precipitate might comprise a mixture of uranyl–hydroxy-hydrates and uranyl carbonates. This surface precipitation mechanism makes it possible to reuse boehmite, by switching the condition to get rid of the precipitated uranium.

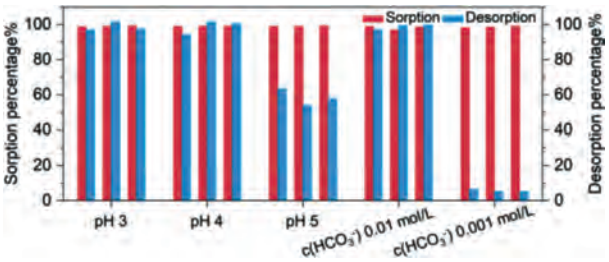

Fig. 9. Effects of desorption conditions on the reusability of boehmite. Each experiment contained three cycles of sorption and desorption with the red bar indicating the sorption efficiency and the blue bar indicating the desorption efficiency (m/v = 0.5 g/L, I = 0.01 mol/L $NaClO_4$, $c(U)_{init.}$ = 71.4 mg/L).

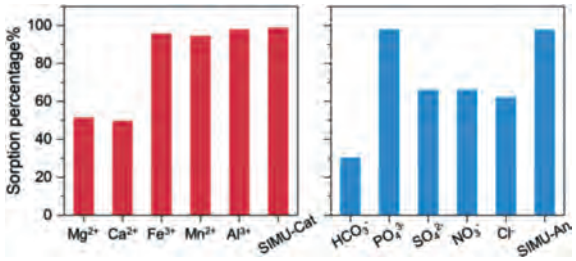

Fig. 10. Uranium removal efficiency of boehmite in a simulated wastewater solution (pH 6.7 ± 0.1, m/v = 0.5 g/L, $c(U)_{init.}$ = 5.9 mg/L).

Five desorption conditions including acid solutions with pH values between 3.0 and 5.0 and alkaline solutions with two bicarbonate concentrations were applied to investigate the reusability of boehmite. Each cycle consisted of a 24-h sorption process and a 12-h desorption process. At the end of each process, the suspension was centrifuged and the supernatant was discarded after recording the uranium concentration. The solution pH in the sorption process was maintained at 6.7 ± 0.1 during the sorption process. As shown in Fig. 9, boehmite showed high sorption efficiency towards uranium with a sorption percentage of about 98% at 6.7 ± 0.1. Both acid and alkaline solutions could effectively recover uranium from the precipitates with a desorption efficiency higher than 97%. However, the desorption efficiency for the acid solution at pH 5.0 was about 57%, and for the alkaline solution with 0.001 mol/L $NaHCO_3$ was less than 6%. In view of these results, one can suggest boehmite as a uranium removal and recovery material since the uranium removal efficiency remained at a high level at 6.7 ± 0.1 and the uranium in the solid phase could be easily recovered by acid or alkaline solutions.

According to the concentrations of cations and anions in the uranium polluted wastewater samples [26,74-76], we prepared simulated samples to investigate the effects of co-existing cations and anions on the uranium removal efficiency by boehmite. The anion was chloride for the simulated cation wastewater samples and the cation was sodium for the simulated anion samples. The effects of each cation and anion were investigated separately, and uranium removal efficiencies by boehmite in the simulated wastewater samples with mixed ions (SIMU-Cat & SIMU-An) were also discussed in Fig. 10. The concentrations of the cations and anions in the simulated wastewater samples are listed in Table 4. The pH 6.7 ± 0.1 of the simulated wastewater and the uranium concentration (5.9 mg/L) were also comparable to the polluted wastewater samples. Mg^{2+} and Ca^{2+} reduced uranium sorption percentage to about 50% possibly through the formation of ternary uranyl carbonates. Fe^{3+}, Mn^{2+} and Al^{3+} increased the sorption percentage to more than 95% because the hydrolyzation precipitation of

Table 3
U 4f binding energy of synthesized minerals after uranium sorption.

	Binding energy (eV)			
	U $4f_{7/2}$	U $4f_{7/2}$ sat.	U $4f_{5/2}$	U $4f_{5/2}$ sat.
Manganite	382.1	384.0	393.0	394.7
Goethite	381.7	383.0	392.6	395.6
Lepidocrocite	381.9	383.8	392.7	394.2

Table 4
The concentrations of cations and anions in the simulated wastewater samples.

Cation	Concentration (mg/L)	Anion	Concentration (mg/L)
Mg^{2+}	98	HCO_3^-	63
Ca^{2+}	15	PO_4^{3-}	5
Fe^{3+}	23	SO_4^{2-}	352
Mn^{2+}	23	NO_3^-	2
Al^{3+}	53	Cl^-	33

the cations at pH 6.7 increased sorption surfaces. In the simulated wastewater with mixed cations, the sorption percentage exceeded 98%. For anions, only phosphate had the promotion effect towards uranium removal with a sorption percentage of 97%. Bicarbonate decreased the sorption percentage to less than 30%. However, the removal efficiency in the simulated wastewater with mixed anions was more than 97%. Boehmite showed excellent uranium removal efficiency in the simulated wastewater samples.

In the current work, with a systematic investigation of uranium sorption on four synthesized minerals (manganite, goethite, lepidocrocite and boehmite), it was unveiled that under acid conditions, the retention ability of Mn- and Fe-oxyhydroxides exceeded Al-oxyhydroxide. Surface complexation was proposed as the predominant mechanism of uranium sorption on manganite, goethite, and lepidocrocite. As for boehmite, surface precipitation of uranyl carbonates and hydrates is the main reason for uranium removal from solution. Moreover, at pH 10.5, carbonate reduced the uranium sorption as the uranyl preferred the soluble carbonate species over surface complexation and precipitation. At pH 5.0, equivalent amount of phosphate could effectively enhance uranium sorption, while the effect of silicate was not apparent unless its concentration was relatively high. Owing to the specific uranium sorption mechanism, boehmite was discovered to be an effective uranium removal material that can be reused by treating with both acid and alkaline solutions. Furthermore, in the simulated wastewater, boehmite also showed outstanding removal efficiency for uranium.

In environment, secondary minerals such as oxyhydroxides exhibit excellent sorption capacity towards uranium when the solution pH was near neutral to sub-alkaline. Uranium sorption on Al-oxyhydroxides is easily influenced by environmental conditions such as pH and the concentration of the co-existing anions, but the uranium surface complexes on Mn- and Fe-oxyhydroxides are relatively stable. Thus, the secondary minerals can play essential roles in the uranium retention at the disposal sites. This work offers critical data of uranium retention in oxyhydroxides, and proposes boehmite as a potential candidate for uranium removal and recovery.

Declaration of competing interest

The authors declare that they have no known competing financial interests or personal relationships that could have appeared to influence the work reported in this paper.

Acknowledgment

Funding for this research was provided by National Natural Science Foundation of China (NSFC, No. 11475008).

Supplementary materials

Supplementary material associated with this article can be found, in the online version, at doi:10.1016/j.cclet.2022.01.019.

References

[1] M. Gavrilescu, L.V. Pavel, I. Cretescu, J. Hazard. Mater. 163 (2009) 475–510.
[2] A. Abdelouas, Elements 2 (2006) 335–341.
[3] H.M. Fernandes, M.R. Franklin, L.H.S. Veiga, et al., J. Environ. Radioact. 30 (1996) 69–95.
[4] C. Chautard, C. Beaucaire, M. Gerard, et al., J. Environ. Radioact. 218 (2020) 106251.
[5] M. Yin, J. Sun, Y. Chen, et al., Environ. Pollut. 244 (2019) 174–181.
[6] Q. Xia, L. Zhang, H. Dong, et al., Geochim. Cosmochim. Acta 279 (2020) 88–106.
[7] Y. Xun, X. Zhang, C. Chen, et al., Bull. Environ. Contam. Toxicol. 100 (2018) 843–848.
[8] Z. Lu, Z. Liu, J. Radioanal. Nucl. Chem. 318 (2018) 923–933.
[9] Z. Wang, H. Qin, X. Liu, Environ. Sci. Pollut. Res. 26 (2019) 5904–5912.
[10] B. Gu, L. Liang, M.J. Dickey, et al., Environ. Sci. Technol. 32 (1998) 3366–3373.
[11] R.A. Crane, M. Dickinson, I.C. Popescu, T.B. Scott, Water Res. 45 (2011) 2931–2942.
[12] J.K. Fredrickson, J.M. Zachara, D.W. Kennedy, et al., Geochim. Cosmochim. Acta 64 (2000) 3085–3098.
[13] X. Pan, Z. Chen, F. Chen, et al., J. Hazard. Mater. 297 (2015) 313–319.
[14] D. Langmuir, Geochim. Cosmochim. Acta 42 (1978) 547–569.
[15] E.J. Elzinga, C.D. Tait, R.J. Reeder, et al., Geochim. Cosmochim. Acta 68 (2004) 2437–2448.
[16] P. Zhang, L. Wang, K. Du, et al., J. Hazard. Mater. 396 (2020) 122731.
[17] Y. Li, L. Xu, P. Bai, et al., Environ. Sci. Nano. 6 (2019) 736–746.
[18] Z. Li, F. Chen, L. Yuan, et al., Chem. Eng. J. 210 (2012) 539–546.
[19] C. Cai, H. Dong, H. Li, et al., Chem. Geol. 236 (2007) 167–179.
[20] Z. Xin, F. Nie, X. Su, et al., Ore Geol. Rev. 127 (2020) 103820.
[21] B. Liu, T. Peng, H. Sun, H. Yue, J. Environ. Radioact. 171 (2017) 160–168.
[22] M. Yin, D.C.W. Tsang, J. Sun, et al., Chemosphere 250 (2020) 126315.
[23] D. Xu, G. Chi, F. Nie, et al., Ore Geol. Rev. 129 (2021) 103944.
[24] K.M. Campbell, T.J. Gallegos, E.R. Landa, Appl. Geochemistry 57 (2015) 206–235.
[25] X. Su, Z. Liu, Y. Yao, Z. Du, Ore Geol. Rev. 127 (2020) 103768.
[26] J. Wang, J. Liu, H. Li, et al., CLEAN - Soil, Air, Water 40 (2012) 1357–1363.
[27] B. Liu, T. Peng, H. Sun, Environ. Sci. Pollut. Res. 24 (2017) 15804–15815.
[28] H.M. Anawar, J. Environ. Manage 158 (2015) 111–121.
[29] A. Abdelouas, W. Lutze, E. Nuttall, J. Contam. Hydrol. 34 (1998) 343–361.
[30] G. Othmane, T. Allard, G. Morin, et al., Environ. Sci. Technol. 47 (2013) 12695–12702.
[31] F. Lahrouch, N. Guo, M.O.J.Y. Hunault, et al., Chemosphere 264 (2021) 128473.
[32] J.G. Reynolds, J. Environ. Sci. Heal. Part A 47 (2012) 2213–2218.
[33] J.E. Post, Proc. Natl. Acad. Sci. U. S. A. 96 (1999) 3447–3454.
[34] P.A. Wilk, D.A. Shaughnessy, R.E. Wilson, H. Nitsche, Environ. Sci. Technol. 39 (2005) 2608–2615.
[35] R.M. Cornell, U. Schwertmann, The Iron Oxides, Wiley, 2003.
[36] Z. Xia, L. Baird, N. Zimmerman, M. Yeager, Appl. Surf. Sci. 416 (2017) 565–573.
[37] D.A. Shaughnessy, H. Nitsche, C.H. Booth, et al., Environ. Sci. Technol. 37 (2003) 3367–3374.
[38] M.A. Islam, M.J. Angove, D.W. Morton, J. Water Process Eng. 32 (2019) 100964.
[39] H. Liu, T. Chen, R.L. Frost, Chemosphere 103 (2014) 1–11.
[40] M. Qin, B. Lu, S. Feng, et al., Chemosphere 230 (2019) 286–293.
[41] D.M. Sherman, C.L. Peacock, C.G. Hubbard, Geochim. Cosmochim. Acta 72 (2008) 298–310.
[42] P.M. Heikkinen, M.L. Räisänen, R.H. Johnson, Mine Water Environ. 28 (2009) 30–49.
[43] B. Peng, A. Piestrzynski, J. Pieczonka, et al., Environ. Geol. 52 (2007) 1277–1296.
[44] T.C. Santini, N.C. Banning, Hydrometallurgy 164 (2016) 38–47.
[45] G.M. Mudd, Environ. Geol. 41 (2001) 390–403.
[46] B.G. Lottermoser, P.M. Ashley, J. Geochemical Explor. 85 (2005) 119–137.
[47] Z. Shi, C. Liu, J.M. Zachara, et al., Environ. Sci. Technol. 43 (2009) 8344–8349.
[48] V.S. Mehta, F. Maillot, Z. Wang, et al., Water Res. 69 (2015) 307–317.
[49] R. Rahnemaie, T. Hiemstra, W.H. van Riemsdijk, J. Colloid Interface Sci. 315 (2007) 415–425.
[50] N. Jordan, N. Marmier, C. Lomenech, et al., J. Colloid Interface Sci. 312 (2007) 224–229.
[51] Y. Jo, A. Kirishima, S. Kimuro, et al., Dalt. Trans. 48 (2019) 6942–6950.
[52] A. Singh, K.U. Ulrich, D.E. Giammar, Geochim. Cosmochim. Acta 74 (2010) 6324–6343.
[53] J. Plášil, Minerals 8 (2018) 551.
[54] X. Zhang, W. Cui, K.L. Page, et al., Cryst. Growth Des. 18 (2018) 3596–3606.

[55] A.J. Frierdich, M.J. Spicuzza, M.M. Scherer, Environ. Sci. Technol. 50 (2016) 6374–6380.
[56] U. Schwertmann, R.M. Cornell, Iron Oxides in the Laboratary, Wiley-VCH Verlag GmbH, Weinheim, 2000.
[57] U. Schwertmann, Iron Soils Clay Miner (1988) 267–308.
[58] Z. Wang, S.W. Lee, J.G. Catalano, et al., Environ. Sci. Technol. 47 (2013) 850–858.
[59] A.S. Kar, A. Saha, A. Chandane, et al., Radiochim. Acta 106 (2017) 191–205.
[60] Y. Ren, H. Bao, Q. Wu, et al., J. Hazard. Mater. 391 (2020) 122207.
[61] M. Wazne, G.P. Korfiatis, X. Meng, Environ. Sci. Technol. 37 (2003) 3619–3624.
[62] S. Doyurum Yusan, S. Akyil Erenturk, Desalination 269 (2011) 58–66.
[63] H. He, K. Alberti, T.L. Barr, J. Klinowski, J. Phys. Chem. 97 (1993) 13703–13707.
[64] J.T. Kloprogge, L.V. D.uong, B.J. Wood, R.L. Frost, J. Colloid Interface Sci. 296 (2006) 572–576.
[65] M. Schindler, F.C. Hawthorne, M.S. Freund, P.C. Burns, Geochim. Cosmochim. Acta 73 (2009) 2471–2487.
[66] E.S. Ilton, P.S. Bagus, Surf. Interface Anal. 43 (2011) 1549–1560.
[67] S. Ardizzone, C.L. Bianchi, D. Tirelli, Colloids Surfaces A: Physicochem. Eng. Asp. 134 (1998) 305–312.
[68] Y. Pei, Q. Chen, Y.C. Xiao, et al., Nano Energy 40 (2017) 566–575.
[69] O.V. Nipruk, G.N. Chernorukov, R.V. Abrazheev, E.L. Kostrova, Inorg. Mater. 53 (2017) 816–819.
[70] T. Allard, P. Ildefonse, C. Beaucaire, G. Calas, Chem. Geol. 158 (1999) 81–103.
[71] A. Froideval, M. Del Nero, C. Gaillard, et al., Geochim. Cosmochim. Acta 70 (2006) 5270–5284.
[72] T. Hattori, T. Saito, K. Ishida, et al., Geochim. Cosmochim. Acta 73 (2009) 5975–5988.
[73] E. Kumar, A. Bhatnagar, W. Hogland, et al., Chem. Eng. J. 241 (2014) 443–456.
[74] P. Li, P. Chen, G. Wang, et al., Chem. Eng. J. 393 (2020) 124819.
[75] P. Yang, S. Li, C. Liu, et al., Sep. Purif. Technol. 263 (2021) 118364.
[76] N. Baumann, T. Arnold, M. Lonschinski, J. Radioanal. Nucl. Chem. 291 (2012) 673–679.